

## ON THE DECAY AND DISAPPEARANCE OF PARAMETRIC ROLL OF SHIPS IN STEEP HEAD WAVES

Dimitris Spanos, spanos@deslab.ntua.gr  
Apostolos Papanikolaou, papa@deslab.ntua.gr

Ship Design Laboratory of the National Technical University of Athens

### ABSTRACT

In an earlier paper the authors highlighted a unique non-linear phenomenon appearing in the parametric rolling of ships in steep waves. According to this, when a ship rolls due to parametric resonance in head waves, and in response to higher wave steepness, the roll amplitude may gradually decrease and may become even zero, meaning practically the disappearance of the parametric resonance phenomenon. This unique non-linear ship response is further discussed in the present paper. It is evidenced that this phenomenon can occur to both smaller and larger ships within practical wave ranges, and it could be explained through the change of the effective  $GM$ , which changes in dependence on the wave steepness as a result of the hydrodynamic ship to wave interaction.

**Keywords:** *Hydrodynamic effects, effective  $GM$ , parametric roll, intact stability, time domain simulation*

### 1. INTRODUCTION

Although the phenomenon of parametric rolling of ships in waves appears well defined in terms of ship intact stability variation, there are still open issues to be clarified, which are related to the complex ship to wave hydrodynamic interaction, and to the way the hydrodynamic effects lead to a variation of ship's stability properties.

Of distinct interest is the non-linear roll response in steep waves, where, though the ship may encounter conditions where parametric roll resonance should be expected, the roll motion can not be sustained. Such behavior could not be explained until now satisfactorily, as some unclear hydrodynamic effect seems to be present and determine such response.

The above roll behavior is detailed in the next sections. It is evidenced that the roll

motion may be limited to waves of moderate steepness, which means that the range of conditions for the occurrence of parametric rolling is limited accordingly. A characteristic relationship between the ship hydrodynamics and the ship stability properties is also identified, which describes the possible mechanism of this roll response.

### 2. DECAY OF ROLL AMPLITUDE IN STEEP WAVES

For a vessel under parametric resonance conditions in regular head waves, the decay of the roll amplitude at the range of higher waves may be expected, as pointed out by Spanos and Papanikolaou (2005, 2006). According to this, when an investigated fishing vessel (length 22 m, displacement 170 tonnes) experienced parametric rolling in head waves and in restrained conditions of three degrees of freedom, namely that of roll, heave and pitch,

then a peak of the roll amplitude resulted for some moderate wave height, whereas for higher waves the roll decreased and even disappeared. This characteristic response is shown in Figure 1, in which the only varying parameter is the wave height and all other parameters are fixed.

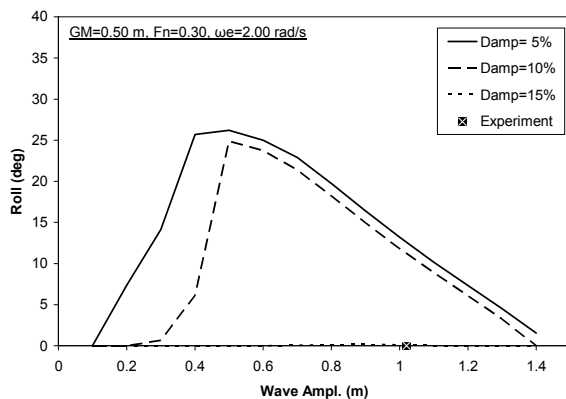


Figure 1. Roll motion amplitude for a fishing vessel, Spanos and Papanikolaou (2006).

The above response could be also identified in the independent theoretical works of Umeda et. al, (2003), Neves and Rodriguez (2006), where sophisticated non-linear roll modelling applied.

Some experimental observation could be found in the published experimental data by Neves et. al (2002). In fact the same fishing vessel (in Figure 1) had been tested in the tank and for a couple of measurements at relatively higher wave steepness the vessel was not rolling.

Examining this behavior for a larger ship, with different hull form characteristics, namely a ROPAX (length 190 m, displacement 22,300 tonnes) by Spanos & Papanikolaou (2006), no decay of roll amplitude was encountered within the investigated range of wave heights up to 6.0 m. However, resonance decay could have been expected for this ship too in even larger waves, as evidenced in the experimental investigation by Hashimoto et. al (2006) for a larger containership ship of similar hull form (length 283 m, displacement 110,000 tonnes). There, an abrupt disappearance of roll for the employed free running post-panamax

containership model occurred for huge wave heights.

Significant experimental evidence for the discussed response could be also found in the tank tests for a large containership (length 300 m) by Lee et. al (2006), where roll stability boundaries have been experimentally determined and the changes in roll could be clearly observed.

In more recent experimental investigations, organized by the authors (HYDRALAB, 2007, SAFEDOR, 2008), the decay of the roll amplitude could be confirmed for the ITTC-A1 containership (length 150 m, displacement 24,000 tonnes), (Umeda et. al, 2000), which has been also studied by ITTC. These tank tests were conducted with the containership model suitably restrained to move in three degrees of freedom, roll, heave and pitch, and consequently they are characterized by lack of uncertainty for the model course and speed keeping.

As presented in Figure 2 below, the tested ITTC-A1 containership was changing the roll behavior for wave heights between 4.8 and 6.0 m. The ship was rolling with amplitude of 15 degrees for a wave height of 4.8 m (steepness,  $H/\lambda \approx 1/37$ ). When the wave increased to 6.0 m ( $H/\lambda \approx 1/30$ ) then no rolling could develop.

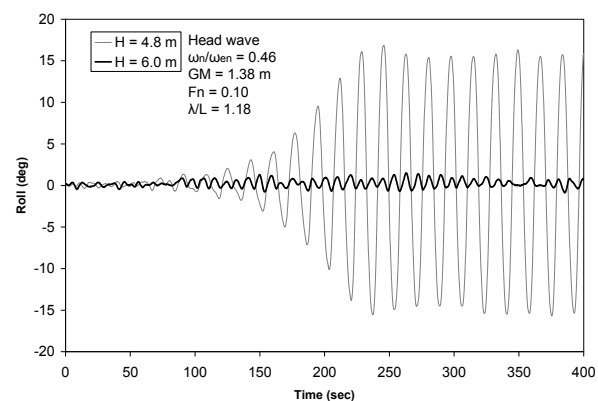


Figure 2. Experimental measurements. Roll disappearance for increased wave height.

Similarly in Figure 3, the ship model could not sustain the roll amplitude when the wave height increased again from 4.8 to 6.0 m.

There, some initial roll motion was triggered externally and the model absorbs this initial disturbance and the roll motion disappears.

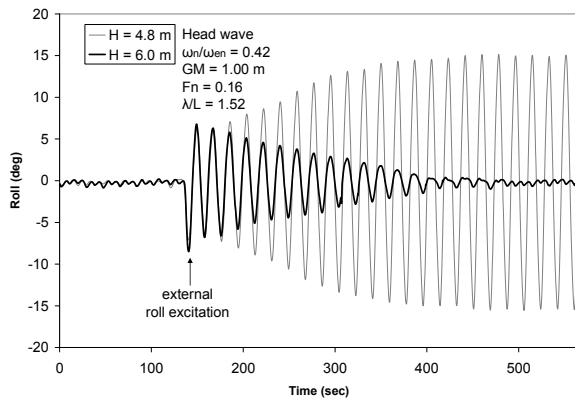


Figure 3. Experimental measurements with external excitation. Roll disappearance for increased wave height.

The roll amplitude of the above conducted model tests is shown in Figure 4, where the experimental measurements are plotted together with corresponding numerical simulation results. Apparently the roll amplitude decays for higher waves and vanishes for heights over 6.0 m ( $H/\lambda \approx 1/30$ ). Since only the wave height is varying in these tests, the increase in height corresponds directly to an increase of steepness ( $H/\lambda$ ). The peak in roll amplitude occurs at a wave height of 3.0 m; when move towards lower waves, then a jump occurs and rolling becomes zero. A second sample at a different frequency is also shown with the dashed line.

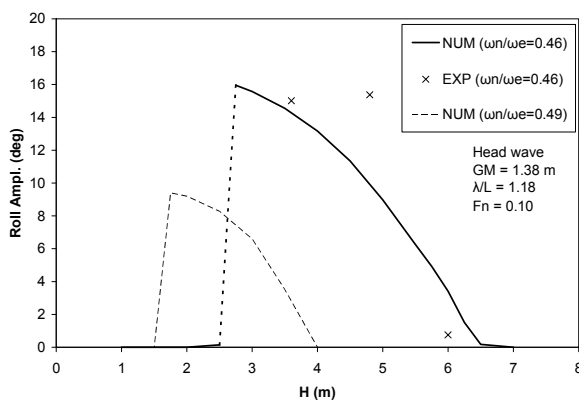


Figure 4. Stationary roll amplitude vs wave height.

The roll response in Figure 4 much resembles a resonance with respect to the wave

height, with a backbone bending to the left. The mechanism of such response and the decay in roll amplitude is discussed below, while the so far experimental evidences support the numerical indications that roll resonance can be limited at moderate wave steepness and such response can be realistic for both small vessels and larger ships, of different hull characteristics.

### 3. THE MECHANISM OF DECAY

The full disappearance of roll motion at steeper waves implies that the observed phenomenon is a result of a change in roll stability and not of some increased roll damping. As, in non-zero rolling, the decrease of roll amplitude could be some damping effect, however, herein it can be excluded.

Since the only variable in the set problem is herein the wave height, whereas all other parameters are fixed (speed, wavelength, hull form, ship loading), it is reasonable to assume that the observed behavior is related to the hydrodynamic forces acting on the ship. Then, the question is of what particular form these forces are that can lead to the observed rolling.

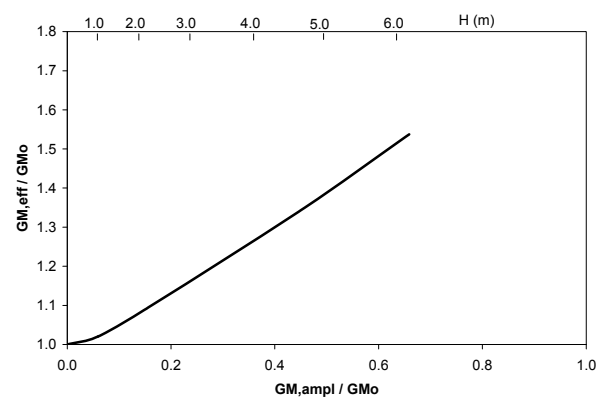


Figure 2. Effective  $GM$  as a function of the  $GM$  variation and wave height.

Systematic numerical simulations of the acting hydrodynamic forces, and their reduction to transverse stability parameters, have revealed the kind of relationship depicted in Figure 5, which is essential for

understanding the mechanism of the phenomenon. The depicted values in Figure 5 are non-dimensionalized with  $GM_o$ , which refers to the still water  $GM$  value.

The effective  $GM_{eff}$  is derived from the uncoupled and undamped form of the roll motion equation (1).

$$I_{xx}\ddot{x} + \Delta GM_o x = M(t) \quad (1)$$

Where  $x$  is the roll and  $t$  is the time. The moment of inertia  $I_{xx}$  includes both structural and hydrodynamic terms, and the moment  $M$  comprises of the time varying roll restoring, the roll damping and the wave excitation. Then setting the total moment acting on the ship as a linear function of roll, the effective  $GM_{eff}$  is defined as time average in equation (2), where  $T$  sufficient long time for convergence of averaging,  $\Delta$  the ship displacement. Correspondingly the  $GM_{ampl}$  is the amplitude of the time varying integrand.

$$GM_{eff} = GM_o - \frac{1}{T} \int_0^T \frac{M(t)}{\Delta x(t)} dt \quad (2)$$

In Figure 5 both the amplitude of variation  $GM_{ampl}$  and the effective  $GM$  increase when the wave height increases (top horizontal axis, non-linear scale). There is an almost linear relationship between  $GM_{eff}$  and  $GM_{ampl}$ , while it is observed that the effective  $GM_{eff}$  changes in the order of  $GM_{ampl}$  change. As a result, at some wave height 6.0 m both  $GM_{eff}$  and  $GM_{ampl}$  have increased approximately by 0.60 m ( $GM_o=1.38$  m).

The relationship of Figure 5 demonstrates that the incurring stability variations are increasingly biased in dependence on the exciting wave height. This asymmetry is related to the hydrodynamic interaction between the ship and incoming waves, and there are two terms already well recognized. The first is the effect of longitudinal ship motion, pitch and heave, and the second is the relative position of the hull with respect to the wave profile.

While the ship pitches in response to the waves the ship stability varies because of the continuous change of the underwater part of the hull. Because of the longitudinal asymmetry of the hull form, for equal pitch by stern and by bow, unequal changes of stability may result, depending on the hull shape at the region around the water plane. This inequality may be low and even negligible for small pitching, while as the waves are getting larger and pitch becomes proportionally larger then these stability bias become gradually more and more intense. Furthermore, the stability variation when the ship lies sequentially on wave crest or trough can also become biased due to the vertical asymmetry of the hull and in relation to the heave motion. Again, when the waves are getting larger this bias becomes more intense.

Therefore, in view of the relationship of Figure 5,  $GM_{eff}$  may continuously increase as the waves increase, and the ship experiences effectively a different  $GM$  to that of still water conditions. With the change of  $GM_{eff}$  then a gradual detune of resonance occurs, and as a consequence a decay in roll amplitude is observed. For even larger wave heights and accordingly larger change of  $GM_{eff}$ , full detune of resonance may result and total disappearance of the roll motion can be observed, like that of Figure 1 and Figure 4.

#### 4. CONSEQUENCES ON ROLL STABILITY

To improve the understanding of the described phenomenon, the relationship for the effective  $GM$  in Figure 5 is explicitly introduced into a simplified roll equation and its consequences on the roll stability are investigated. This approach is free of complex details that might be introduced when employ the time-domain numerical simulation.

For a ship in regular head waves, let us assume an uncoupled and undamped roll equation with time varying restoring.

$$I_{xx}\ddot{x} + \Delta GM(t)x = 0 \quad (3)$$

where the symbols denote,  $x$  the roll,  $I_{xx}$  the mass moment of inertia,  $\Delta$  the ship displacement,  $GM$  the metacentric height and  $t$  the time.

Assuming also a sinusoidal time variation for roll restoring, like Grim (1952)<sup>1</sup>, then the roll equation becomes

$$I_{xx}\ddot{x} + \Delta(GM + GM_a \cos \omega t)x = 0 \quad (4)$$

where  $GM_a$  is the amplitude of time variation of  $GM$  and  $\omega$  the frequency of variation.

Equation (4) may be written in concise form as below

$$\ddot{x} + (\alpha + \beta \cos \omega t)x = 0 \quad (5)$$

$$\text{where } \alpha = \frac{\Delta GM}{\omega^2 I_{xx}} = \left( \frac{\omega_n}{\omega} \right)^2 \quad \beta = \frac{\Delta GM_a}{\omega^2 I_{xx}}$$

The parameter  $\alpha$  expresses the ratio of the frequency of variation  $\omega$  to the natural frequency  $\omega_n$ , and the parameter  $\beta$  expresses the magnitude of the stability variation.

In accordance to the discussion of the previous section,  $\alpha$  is herein expressed with respect to the effective  $GM_{eff}$ . And taking into account a linear dependence to  $GM_a$ , as evidenced in Figure 5, then  $\alpha$  can be written in the form

$$\alpha = \alpha_o + k\beta \quad (6)$$

where  $\alpha_o = \frac{\Delta GM_o}{\omega^2 I_{xx}}$ ,  $GM_o$  refers to the calm water GM and  $k$  is the linearity coefficient. Then inserting (6) into (5) it is obtained

$$\ddot{x} + [\alpha_o + \beta(k + \cos \omega t)]x = 0 \quad (7)$$

Thus the coupling of the two parameters  $\alpha$  and  $\beta$  has been explicitly included in the

equation of the roll motion. Equation (7) is herein called *conditional* roll equation to distinguish it from ordinary equation (5). This equation is still a Mathieu type differential equation like (5), while having modified the constant term  $\alpha$ .

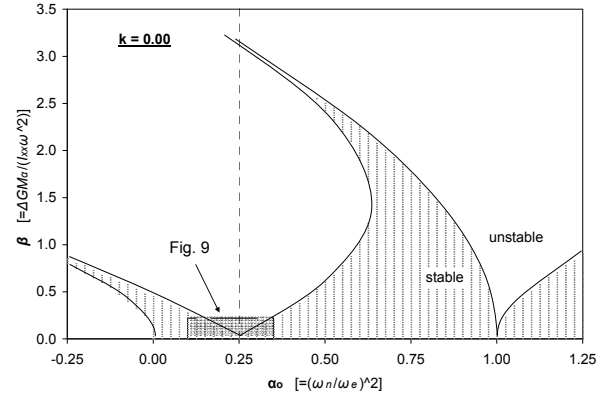


Figure 6. Stability diagram of the ordinary roll (Mathieu) equation.

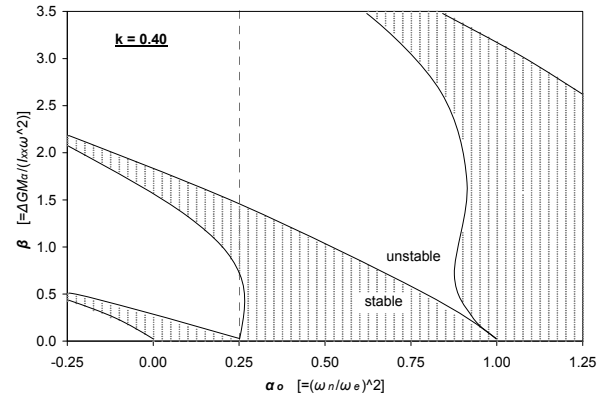


Figure 7. Stability diagram of the conditional roll equation.

Next, the stability of the equation (7) is presented in comparison to the stability of the ordinary roll equation (5); focus is placed on the region of the first parametric resonance, which is of practical interest for the ships in waves.

Above Figure 6 shows the stability of the basic roll equation (5), where the shaded region corresponds to the stable and the white to unstable roll conditions. This is the stability diagram of the ordinary Mathieu equation. At the first parametric resonance  $\alpha_o = 0.25$  instability is apparent throughout the parameter  $\beta$  with an exception for the very narrow region around  $\beta = 3.0$  (where the dashed line intersects

<sup>1</sup> Grim (1952) dealt thoroughly with the parametric roll phenomenon on the basis of the Mathieu equation and ship model experiments in which the  $GM$  could be varied systematically; the effect of waves, and ship motions, on  $GM$  variations was later investigated and experimentally confirmed by Paulling (1961).



the thin top edge of stable region). This region is too small and too far away from the range of practical interest. In this diagram the range of interest (where the ship responses occur) is limited within the shaded square, which is discussed later in Figure 9.

Figure 7 presents the stability diagram of the conditional roll equation (7) and for a value  $k=0.40$ . Qualitatively the shape of the stable regions remains similar to the one of Figure 6, with the difference that here they have bended to the left side. The higher  $k$  constant is the more intensive bending to the left occurs. As a consequence of that bending a stable region results along the first parametric resonance ( $\alpha_o=0.25$ ) between  $0.8<\beta<1.5$ , which is closer (however still far) to the practical range of  $\beta<0.15$  (next Figure 8, Figure 9). The unstable conditions are limited to  $\beta<0.8$ , which corresponds to the lower stability variations namely lower wave heights.

Focusing now to the region  $\beta<0.15$  and for  $k=0.80$  (which corresponds to the actual ship data of Figure 5) the stability of equation (7) takes the form of Figure 8.

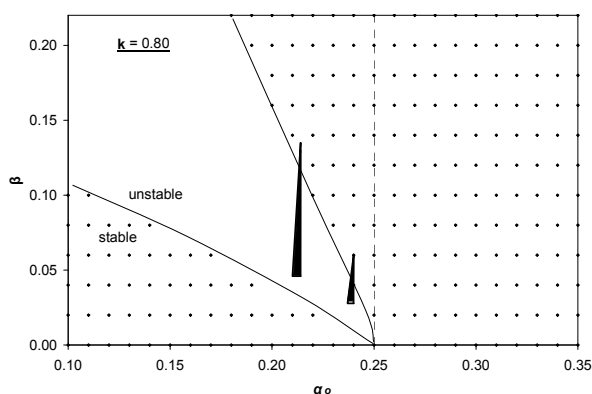


Figure 8. Stability diagram of the conditional roll eq. and time-domain simulation resonance.

The stable regions have strongly bended to the left, resulting to full stability along the dashed line at the dominant resonance  $\alpha_o=0.25$ . The two vertical line segments (at  $\alpha_o=0.21$  and  $0.24$ ) correspond to the range of the roll resonance for the containership as discussed in Figure 4. The roll amplitude is finite along these segments, and the arrows of varying

thickness denote the gradual decrease of the roll. They have resulted from time domain simulation of the ship motion in waves, and they are limited between the stability boundaries of equation (7).

The resulting upper stability boundary of the used simplified roll model is a clear border between stable and unstable conditions, whereas for the more realistic conditions produced with the numerical time domain simulations, a transition from instability to stability results. The stability boundaries of the two theoretical methods (the roll equation (7) and the time domain simulation) apparently converge, which indicates that the essential cause of the discussed phenomenon has been well captured by time domain simulation and reproduced with the simplified roll equation.

In Figure 8, the parametric resonance is apparently bounded to values  $\alpha_o<0.25$  ( $\omega_n/\omega_e<0.5$ ). This also explains the empirical knowledge from tank model tests where parametric roll resonance is detected at slightly higher frequencies of encounter compared to the double of the natural frequency, which is specified by the theoretical condition ( $\omega_n/\omega_e=0.5$ ). It can be observed that the tank tests sampled in Figure 2 and Figure 3 have been carried out at  $\omega_n/\omega_e=0.46$  and  $0.42$  respectively.

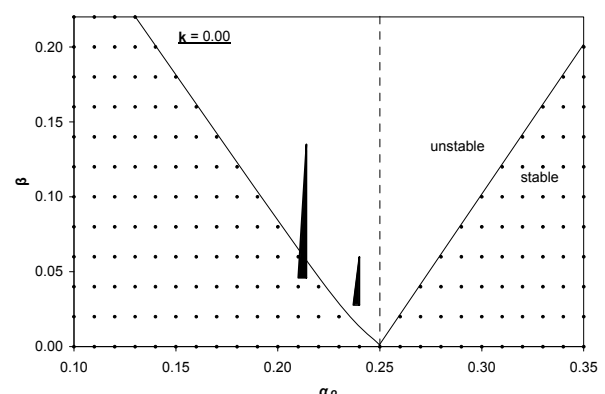


Figure 9. Stability diagram of the ordinary roll eq. and time-domain simulation resonance.

To emphasize the bending of the stability regions of Figure 8 due to the change of the effective  $GM_{eff}$ , the above Figure 9 presents the

two samples of resonance ranges together with the stability of the ordinary roll equation (5) (which is the focus of Figure 6 at first resonance). Here,  $k=0.0$ , namely a constant effective  $GM$  throughout the wave range is assumed, and then, no decay of the roll amplitude would be expected at steeper waves.

According to the present analysis, the decay and disappearance of the roll amplitude in steeper waves has been attributed to the non-zero  $k$  parameter of the relationship (6), namely the continuous increase of the effective  $GM$  over the wave steepness, while a consequence of the non-zero  $k$  on the roll stability is the bending of the stability regions. The parameter  $k$  is an endogenous parameter of the *ship in waves* hydrodynamic system. It depends on the hydrodynamic properties of ship, as determined by the hull form, and particularly on the hull shape around the still water plane, the ship loading and the wave hydrodynamics.

The above is demonstrated in Figure 10, which shows the effect of the wavelength on the magnitude of the roll amplitude for the containership. The curves correspond to different wavelengths, while the resonance condition of  $\omega_n/\omega_e=0.46$  is kept constant for all cases by change of the forward speed. All cases correspond to a constant value  $\alpha_o=0.21$  in equation (7).

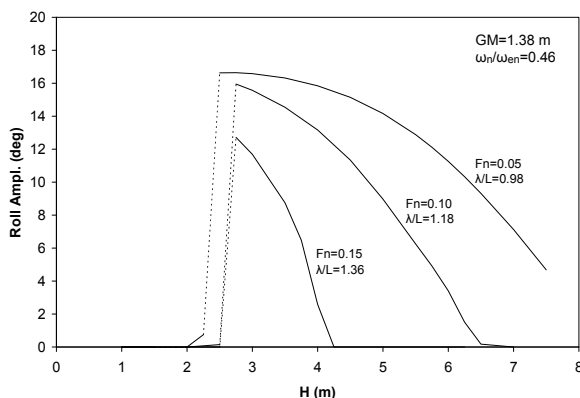


Figure 10. Roll resonance for varying wavelength-speed.

The resonance becomes stronger for the shorter wavelength (simultaneously lower

speed), and the resonance gradually decreases for the longer wavelength (higher speed). In view of the current analysis the difference of the three curves implies some difference for the  $k$ -parameter of  $GM$  effective. In Figure 8, the upper stability boundary should have become lower when ship advances in the longer wave.

Indeed, as presented in Figure 11, the  $k$  parameter (the curves' slope) is getting higher for the longer waves. The herein observed difference is attributed to the increased pitch when advancing through the longer wave. Regardless of specific reasons, the ship to wave hydrodynamic interaction results to the described characteristic change of the ship's transverse stability, namely that of the effective  $GM$ .

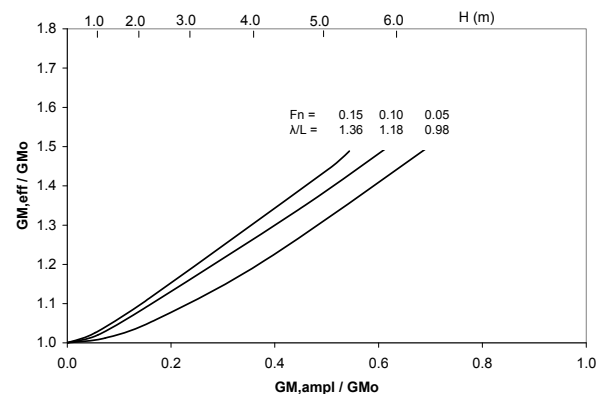


Figure 11. Effective  $GM$  (for cases of Figure 10).

## 5. CONCLUSIONS

The investigation presented confirms that the parametric rolling of ships in regular head waves may decay and even disappear in steeper waves. This can be expected for both small vessels and larger ships within waves of practical range.

The phenomenon could be explained with the change of the effective  $GM$ , which gradually increases as the wave height increases too. Over some wave steepness the ship and the incoming wave are away of resonance tune and as a consequence the roll amplitude decreases and may disappear.



It was also presented that the effective  $GM$  and the variation of  $GM$  can be satisfactorily correlated with a linear relationship, which is the result of the hydrodynamic forces acting on the ship. This relationship proved to be essential for the ship roll stability, by comparative studies between the two employed theoretical methods, namely that of the time domain numerical simulation (with coupled heave, roll and pitch) and that of the uncoupled roll equation.

Finally, the investigation for a generic modeling of the effective  $GM$  in relation to the ship hull form and waves characteristics that would greatly help ship designers and operators in assessing ship's stability in waves is considered an interesting subject for future development.

## 6. ACKNOWLEDGEMENTS

The presented investigation has been partially supported by the European Commission under the FP6 Sustainable Surface Transport Programme, the Integrated project SAFEDOR (Design, Operation and Regulation for Safety) Contract No. FP6-IP-516278. The European Community and the authors shall not in any way be liable or responsible for the use of any such knowledge, information or data, or of the consequences thereof.

## 7. REFERENCES

- Grim, O., Roll Motions, Stability and Safety in Seaways, *Journal Schiffstechnik*, Vol. 1, 1952, 10-21, (in German).
- Hashimoto, H., Umeda, N., Matsuda, A., Nakamura, S., 2006, Experimental and Numerical Studies on Parametric Roll of a Post-Panamax Container Ship in Irregular Waves, *Proc. of 9th Inter. Conf. of Stability of Ships and Ocean Waves*, Rio de Janeiro.
- HYDRALAB III, Ship Model Tests in Parametric Roll in Natural Seas, HyIII-CEH-5. FP6 EC Integrated Infrastructure Initiative HYDRALAB III, Access to major experimental ship hydrodynamics and ice engineering facilities, CEHIPAR, El Pardo, Nov. 2007.
- Lee, H.-H., Lee I.-H., Lee Y.-W., Yoon, M.-T., 2006, Experimental and Numerical Investigation into the Parametric Roll Resonance in Head Seas for an Ultra Large Containership, *Proc. of 9th Inter. Marine Design Conference*, Ann Arbor, MI, USA.
- Neves, M. and Rodriguez, C., An Investigation on Roll Parametric Resonance in Regular Waves, *Proc. of 9th Inter. Conf. on Stability of Ships and Ocean Vehicles*, Brazil, 2006.
- Neves, M., Perez, N., Lorca, O., Experimental Analysis on Parametric Resonance for Two Fishing Vessels in Head Seas, *Proc. of 6th Inter. Ship Stability Workshop*, Webb Institute, NY, USA, Oct. 13-16, 2002.
- Paulling, J. R., The Transverse Stability of a Ship in a Longitudinal Seaway, *Journal of Ship Research*, Vol. 4, No. 4, 1961.
- SAFEDOR, Ship model Tests on Parametric Rolling in Waves, European research project SAFEDOR (Design, Operation and Regulation for Safety), SP.7.3.9, FP6 Sustainable Surface Transport Programme, INSEAN, Rome, Sep. 2008.
- Spanos, D. and Papanikolaou, A., Numerical Simulation of a Fishing Vessel in Parametric Roll in Head Seas, *Proc. of 8th Inter. Workshop on Stability and Operational Safety of Ships*, Istanbul, Turkey, October 6-7, 2005.
- Spanos, D. and Papanikolaou, A., Numerical Simulation of Parametric Roll in Head Seas, *Proc. of the 9th Inter. Conf. of Stability of Ships and Ocean Waves*, Rio de Janeiro, 2006.
- Umeda, N., A. Munif and H. Hashimoto, Numerical Prediction of Extreme Motions and Capsizing for Intact Ships in Following/ Quartering Seas, *Proc. of the 4th Osaka Colloquium on Seakeeping Performance of Ships*, Osaka, Oct., 2000, 368-373.